Research Article

Molecular Modeling Suggests Conformational Scaffolds Specifically Targeting Five Subtypes of Somatostatin Receptors

Gregory V. Nikiforovich[1],*, Garland R. Marshall[1] and Samuel Achilefu[2]

[1]Department of Biochemistry and Molecular Biology, Washington University Medical School, St. Louis, MO 63110, USA
[2]Department of Radiology, Washington University Medical School, St. Louis, MO 63110, USA
*Corresponding author: Gregory V. Nikiforovich, gregory@ccb.wustl.edu

Several analogs of somatostatin with conformational constraints in their peptide backbones have been modeled to determine energetically feasible conformations. Comparison of low-energy backbone structures of these peptides suggested unique conformations of the central Phe/Ala$_i$-D-Trp$_{i+1}$-Lys$_{i+2}$-Thr$_{i+3}$ fragment characteristic for specific interactions of somatostatin with each of the five distinct subtypes of somatostatin receptors (SSTRs). The conformations obtained were in good agreement with experimental data obtained earlier by NMR measurements and/or X-ray crystallography. The results help rationalize experimental observations on the specificity of binding of various somatostatin analogs with different subtypes of the SSTRs. They also serve as templates for the design of conformationally constrained non-peptide scaffolds that effectively and selectively interact with different subtypes of SSTRs. Such scaffolds can be convenient carriers of radiolabels and near-infrared labels in specific agents for imaging tumors expressing different SSTR subtypes.

The naturally occurring cyclopeptide somatostatin-14 (H-Ala[1]-Gly[2]-*cyclo* [Cys[3]-Lys[4]-Asn[5]-Phe[6]-Phe[7]-Trp[8]-Lys[9]-Thr[10]-Phe[11]-Thr[12]-Ser[13]-Cys[14]]-OH) is expressed in brain and in most peripherical organs and tissues, and participates in a wide variety of physiological processes. Currently, five distinct subtypes of G-protein-coupled receptors highly specific for somatostatin have been cloned and characterized (SSTR1 to SSTR5). Importantly, some SSTR subtypes are overexpressed in tumors, such as gastroenteropancreatic, pituit-

ary and carcinoid tumors (1). While most tumors show overexpression of SSTR2 (breast cancer, carcinoid, neuroblastoma, *etc.*), some tumors also overexpress SSTR5 (GH-expressing pituitary adenoma and kidney cancer), or SSTR4 (ovary cancer), or even SSTR1, SSTR2, SSTR3 and SSTR5 simultaneously (thyroid cancer) (1,2).

Recently, many studies focused on discovering novel analogs of somatostatin that specifically target each of the SSTR subtypes for therapeutic and diagnostic purposes in oncology. For instance, octapeptides related to octreotide (sandostatin), D-Phe-*cyclo*[Cys-Phe-D-Trp-Lys-Thr-Cys]-Thr-*ol*, are used clinically as anti-proliferation drugs as well as radiopharmaceuticals for imaging neuroendocrine tumors [e.g., (1,2) and references therein]. In addition, conjugation of the peptides to near-infrared fluorescent molecular probes extends their use in molecular optical imaging (3–5). However, octreotide-related peptides remain of limited use because they interact primarily only with SSTR2/SSTR5 and not other subtypes of SSTRs.

Several hundreds of peptide analogs have been synthesized and tested to study structure-activity relationships for somatostatin during the past three decades (for a brief review see (6,7)). In recent years, somatostatin analogs with high selectivity for each subtype of different SSTRs have been developed (8–17). Extensive NMR measurements (7,11,15,17,18) and X-ray crystallography studies (19) were performed to generate 3D models of the specific somatostatin pharmacophore for each subtype of the SSTRs. The results suggested that different specific spatial arrangements of the aromatic and lysine side chains in the central fragment of somatostatin, Phe[7]-Trp[8]-Lys[9]-Thr[10], facilitate specific interactions of the peptide with SSTR1 (11), SSTR2 (7,19), SSTR2/SSTR3/SSTR5 (7), SSTR3 (17) and SSTR4 (15). Also, non-peptide compounds selective to each subtype of SSTRs were developed based on combinatorial libraries and high-throughput screening (20).

At the same time, rational design of non-peptide compounds specific for a given subtype of different SSTRs would significantly benefit from the knowledge of possible privileged scaffolds for incorporating and orienting the side chains in specific spatial arrangements. This has been exemplified by the development of sugar-based somatostatin-related compounds (21). In this regard, knowledge of the backbone conformations of the central fragment of somatostatin that are specific for interaction with each subtype of SSTRs would be especially valuable, because these conformations may serve as convenient templates for further development of non-peptide scaffolds [see (22,23)]. Therefore, we performed mode-

ling studies for several analogs of somatostatin with conformational constraints in their peptide backbones to determine, where possible, conformations of the peptide backbone for the central tetrapeptide in somatostatin (corresponding to the sequence Phe[7]-Trp[8]-Lys[9]-Thr[10]), which are responsible for specific interactions with each of the five different subtypes of SSTRs.

Methods and Materials

The force field used in energy calculations was the ECEPP/2 force field (24,25) with rigid valence geometry and planar *trans*-peptide groups (the ω angles were allowed to vary within the cyclic peptides). The Lys side chains were considered charged. Aliphatic and aromatic hydrogens were generally included in united atomic centers of CH_n type. H^α-atoms and amide hydrogens were described explicitly, as well as hydrogens in the N-methyl fragments. Energy calculations were performed with the value of the macroscopic dielectric constant $\varepsilon = 80$ to mimic the water environment. To close the disulfide cycles, parabolic closing potentials with U_0 of 100 kcal/mol were added to interactions between the sulfur atoms of cysteines, and with U_0 of 10 kcal/mol to interactions between the sulfur atom of the first cysteine and the $C\beta$ atom of the second one. Valence geometry of the N-methyl residues was derived from the available crystal data; partial atomic charges were calculated by the use of the SYBYL program (the Gasteiger–Huckel method).

Conformational sampling for peptide backbones was performed in several steps employing all combinations of local minima for the ϕ, Ψ values at the Ramachandran map for the L-amino acid residues, namely (−140°, 140°), (−75°, 140°), (−75°, 80°), (−60°, −60°), and (60°, 60°). For D-Trp and D-Phe, the same minima with the opposite signs of dihedral angle values were employed. For N-methylated amino acid residues, both sets of local minima (i.e., as for L- and for D-amino acid residues) were considered. At the first step of calculations, all combinations of local minima allowing spatial arrangements of the $C\beta$ atoms of cysteines at distances less

than 6 Å were selected. Then, energy calculations were performed for each selected conformation of the disulfide cycles. Conformations satisfying energy cut-off $\Delta E = E_i − E_{min} < 10$ kcal/mol (compounds **1–8**, see Table 1) were selected for further steps. For compounds **9–12** (Table 1), this step was the final one, and final selection of low-energy conformers was performed with energy cut-off of 8 kcal/mol. For compounds **1–8**, the residues flanking the disulfide cycle were added at the final step, and low-energy conformations were then selected with energy cut-off of 8 kcal/mol. The dihedral angle values of side chain groups and of terminal groups of the backbone were optimized at every step before energy minimization to achieve their most favorable spatial arrangements employing an algorithm described earlier (26). Redundant backbone conformations were removed at each step as follows: if one (or more) of the backbone torsion angles differed by more than 40° from the corresponding angle of any other low-energy conformation, the backbone was considered unique (non-redundant); otherwise it was removed.

Results and Discussion

Somatostatin analogs selected for modeling in our study are listed in Table 1, which includes information on their binding to the five subtypes of SSTRs. We have selected two main series of octapeptides, namely compounds **1–8** with internal hexapeptide cycle (27) and compounds **9–12** that are cyclic octapeptides (15). Compounds **1–8** retain the same side chains throughout the series; therefore, their differences in binding to different subtypes of SSTRs may be attributed solely to changes in backbone conformations due to N-methylation of each sequential residue (shown in bold in Table 1). Similarly, differences in binding between compounds **9–10** or **11–12** may be attributed to replacements of the Trp residue with its enantiomer. Importantly, each of the series (compounds **1–8** and **9–12**, respectively) was tested in the same experimental systems with the corresponding radioligand binding assays [see (27,28)]. Also, nearly all peptides in Table 1 contained the same side chains

Table 1: Somatostatin analogs with conformational restraints in the peptide backbone selected for modeling in the present study. Amino acid replacements in compounds 2–12 compared to compound 1 are shown in bold, as well as the K_d or IC_{50} values that were lower than 100 nM

Compd	Sequence	K_d or IC_{50}, nM[a]					Number of low-energy conformers
		SSTR1	SSTR2	SSTR3	SSTR4	SSTR5	
1	D-Phe-c[Cys-Phe-D-Trp-Lys-Thr-Cys]-Thr-NH2	761	**0.15**	**11.84**	>1000	**8.35**	236
2	D-Phe-c[**N-Me-Cys**-Phe-D-Trp-Lys-Thr-Cys]-Thr-NH2	378	**1.04**	**13**	>1000	**23.71**	105
3	D-Phe-c[Cys-**N-Me-Phe**-D-Trp-Lys-Thr-Cys]-Thr-NH2	>1000	**13.17**	830	>1000	**83.24**	74
4	D-Phe-c[Cys-Phe-**N-Me-D-Trp**-Lys-Thr-Cys]-Thr-NH2	1200	**23.5**	**11.05**	>1000	**0.61**	57
5	D-Phe-c[Cys-Phe-D-Trp-**N-Me-Lys**-Thr-Cys]-Thr-NH2	867	**1.84**	67.48	>1000	**8.41**	96
6	D-Phe-c[Cys-Phe-D-Trp-Lys-**N-Me-Thr**-Cys]-Thr-NH2	>1000	>1000	>1000	>1000	>1000	17
7	D-Phe-c[Cys-Phe-D-Trp-Lys-Thr-**N-Me-Cys**]-Thr-NH2	622	**56.23**	**44.4**	574	**28.42**	106
8	D-Phe-c[Cys-Phe-D-Trp-Lys-Thr-Cys]-**N-Me-Thr**-NH2	>1000	**14.84**	124.3	182	313	152
9	H-c[Cys-Phe-Phe-**Trp**-Lys-Thr-Phe-Cys]-OH	**5.3**	130	**13**	**0.7**	**14**	201
10	H-c[Cys-Phe-Phe-D-Trp-Lys-Thr-Phe-Cys]-OH	**27**	**41**	**13**	**1.8**	**46**	169
11	H-c[Cys-Phe-**Ala**-**Trp**-Lys-Thr-**Ala**-Cys]-OH	>1000	>1000	>1000	**3.5**	>1000	78
12	H-c[Cys-Phe-**Ala**-DTrp-Lys-Thr-**Ala**-Cys]-OH	>1000	>1000	>1000	**9.5**	>1000	34

[a]K_d for compounds 1–8 [ref. (27)] and IC_{50} for compounds 9–12 [ref. (15)].

in the central tetrapeptide prototyped by the sequence Phe-D-Trp-Lys-Thr, with the only exception being compounds **11–12** (Ala instead of Phe). Additionally, Table 1 presents the total numbers of low-energy conformations of the peptide backbone (those satisfying to the chosen energy cut-off, see section Methods and Materials) for each of compounds **1–12**.

The binding data for compounds **1–12** in Table 1 could be roughly divided into two classes, namely those with K_d or IC_{50} values smaller than 100 nM (shown in bold in Table 1), and those with the values greater than 100 nM. We assumed that, when the level of binding for a given compound to a given subtype of SSTRs falls into the first class, the compound effectively interacts with this particular SSTR subtype. Since effective interaction of peptide ligand with the specific receptor requires distinct shape complementarity of ligand and receptor, the division of the binding data into two wide classes may allow selection of low-energy conformations of the peptide backbone characteristic for interaction with different SSTR subtypes. For instance, backbone conformations specific for interactions with SSTR1 should be geometrically similar for compounds **9** and **10** (the corresponding IC_{50} values being 5.3 nM and 27 nM, respectively; see Table 1) and, at the same time, non-similar to all low-energy conformations of all other compounds (the corresponding IC_{50} values being at least 378 nM; see Table 1). Conformations specific for interactions with SSTR2 should be similar for compounds **1, 2, 3, 4, 5, 7, 8** and **10**, but not similar to any conformation of compounds **6, 9, 11** and **12**. For interactions with SSTR3, one can expect similarity of conformations for compounds **1, 2, 4, 5, 7, 9** and **10**, which would be non-similar to conformations of compounds **3, 6, 8, 11** and **12**. For interactions with SSTR4, geometrical similarity may be required for some conformations of compounds **9–12**, but not for those of compounds **1–8**. Finally, effective interactions with SSTR5 may be expected for conformations similar for compounds **1, 2, 3, 4, 5, 7, 9** and **10**, and non-similar to conformations of compounds **6, 8, 11** and **12**.

Each of the low-energy conformations found for compounds **1–12** were compared with each other in order to establish geometrical similarity or non-similarity between them. First, the $C\alpha$–$C\beta$ vectors (those defining the general orientation of side chains) of the hexapeptide fragments prototyped by sequences Cys-Phe-D-Trp-Lys-Thr-Cys for compounds **1–8** and Phe-Phe/Ala-D-Trp/Trp-Lys-Thr-Phe/Ala for compounds **9–12** were overlapped and the corresponding rms values for $C\alpha$ and $C\beta$ atoms calculated. At this step, it was important to establish reasonable values of the rms cut-offs for discrimination of geometrically similar and non-similar conformations. Obviously, too loose cut-off values might not allow discrimination between similar and non-similar conformations, whereas too stringent values might not allow identification of similar conformations in different compounds effectively interacting with the same subtype of SSTRs. After adjusting the cut-off values, we decided to employ a 'similarity' rms cut-off of 1.5 Å, and a 'non-similarity' cut-off of 1 Å. These values ensured that determination of similar and non-similar groups of conformations for compounds **1–12** was in accordance with requirements for their specific interactions with SSTR subtypes. At the last stage of comparison, groups of conformations determined as similar from the point of view of specific interactions with each SSTR subtype were overlapped by all heavy atoms of the peptide backbones for the hexapeptide fragments (including $C\beta$ atoms) and divided into several clusters by an rms cut-off of 1 Å.

Generally, geometrical comparison was able to determine five groups of conformations geometrically similar for some compounds and non-similar for other compounds in accordance with their pattern of specific interactions with five different subtypes of SSTRs as described in Table 1. Conformations specific for interactions with SSTR2, SSTR3 and SSTR5 were selected first for compound **4**, which possessed the smallest set of low-energy conformations for the peptide backbone (57 conformations) among compounds interacting only with SSTR2, SSTR3 and SSTR5 (see Table 1). Geometrical comparison selected 25 of the 57 low-energy conformations as those capable to interact with SSTR2, 17 with SSTR3, and 9 with SSTR5. However, these groups of conformations were intersecting, leaving only 18 conformations presumably interacting specifically with SSTR2 and 8 with SSTR3. At the same time, all 9 conformations selected as interacting with SSTR5 were also selected as those interacting either with SSTR2 or SSTR3. In other words, some low-energy conformations of compound **4** may interact with all three receptor subtypes (SSTR2, SSTR3 and SSTR5), whereas some may interact either only with SSTR2 or only with SSTR3. It would be logical to assume that conformations of compound **4** may rather easily be interconverted when interacting with the specific subtype of SSTRs, which makes compound **4** specific to SSTR2/3/5, but not to each individual receptor subtype. The same pattern was observed also for all other compounds interacting with SSTR2, SSTR3 and SSTR5 (compounds **1, 2, 5** and **7**). Groups of low-energy conformers characteristic for SSTR1 and SSTR4 were selected first for compounds **10** and **12**, the former being non-specific, and the latter being SSTR4-specific (see Table 1). Fifteen conformations of compound **10** were determined as those interacting with SSTR1, and 10 conformations of compound **12** were determined as those interacting with SSTR4. There was no intersection between the two groups, which indicated that selectivity of interaction of compound **12** with SSTR4 may be not only due to replacement of the Phe side chains with Ala (as compared with compound **10**), but also due to specific backbone conformations.

It was also possible to distinguish the dihedral angle values characteristic for conformations most typical for interactions with different subtypes of SSTRs. The angle values were determined for compound **1** (for SSTR2, SSTR3 and SSTR5) and compounds **10** and **12** (for SSTR1 and SSTR4). To determine these values, we assumed that typical conformations, first, should belong to the most populated clusters in the corresponding compounds, and, second, that the average values for any dihedral angle of the peptide backbone in the central tetrapeptide fragment interacting with different SSTRs should be as different as possible. Table 2 lists the dihedral angles of the peptide backbone of fragment Phe_i-D-Trp_{i+1}-Lys_{i+2}-Thr_{i+3} in compounds **1** and **10** (or fragment Ala_i-D-Trp_{i+1}-Lys_{i+2}-Thr_{i+3} in compound **12**) which, according to these results, may represent conformations effectively interacting with SSTR1-5. The values of dihedral angles in Table 2 were averaged over the most populated clusters in the corresponding compounds. Since there were two equally populated clusters of compound **1** typical for interaction with SSTR5, Table 2 contains both conformations for this case. The

		Phe/Ala		D-Trp		Lys		Thr	
Compd	Receptor	ϕ	Ψ	ϕ	Ψ	ϕ	Ψ	ϕ	Ψ
10	SSTR1	−103 ± 12	−10 ± 20	98 ± 30	−122 ±13	−93 ± 17	−10 ± 21	−82 ± 6	−18 ± 58
1	SSTR2	−154 ± 3	140 ± 23	62 ± 6	−119 ± 5	−118 ± 20	8 ± 27	−145 ± 8	145 ± 12
1	SSTR3	−148 ± 8	142 ± 15	28 ± 57	−109 ± 39	−72 ± 2	−40 ± 11	−88 ± 14	102± 18
12	SSTR4	−81 ± 5	118 ± 4	93 ± 4	52 ± 1	−145 ± 1	139 ± 1	−70 ± 4	−39 ± 3
1	SSTR5 (1)	−120 ± 12	162 ± 1	−57 ± 1	−41 ± 0	−70 ± 3	−58 ±2	−144 ± 6	143 ± 8
1	SSTR5 (2)	−88 ± 3	159 ± 7	−57 ± 0	−42 ± 3	−77 ± 5	−29 ± 5	−86 ± 4	−32 ± 1

Table 2: Average values and standard deviations for the dihedral angles of peptide backbone in the central tetrapeptide of somatostatin-related peptides characteristic for specific interactions with subtypes of SSTRs

typical conformations which, according to our results, are characteristic for specific interactions with different SSTRs are depicted in Figure 1 for compounds **1**, **10** and **12**.

The average dihedral angle values listed in Table 2 show the presence of various β-turn reversals in different SSTR-subtype-specific conformations of the central tetrapeptide of somatostatin. For instance, both SSTR1- and SSTR2-specific conformations feature a distinct βII' turn at the D-Trp$_{i+1}$-Lys$_{i+2}$ dipeptide fragment [the standard values being $\phi_{i+1} = 60°$, $\Psi_{i+1} = −120°$; $\phi_{i+2} = −80°$, $\Psi_{i+2} = 0°$ (29)], but the Ψ values for the Phe$_i$ residue are drastically different in the two conformations. It is clearly seen in Figure 2, where orientations of this residue in SSTR1-specific and SSTR2-specific conformations are almost opposite. In both conformations

suggested as specific for interactions with SSTR5, the D-Trp$_{i+1}$-Lys$_{i+2}$ dipeptide possesses another type of the β-turn, βIII [the standard values $\phi_{i+1} = −60°$, $\Psi_{i+1} = −30°$; $\phi_{i+2} = −60°$, $\Psi_{i+2} = −30°$ (29)]. Since conformations specific for interactions with SSTR3 were characterized by fairly wide standard deviation for ϕ_{i+1} (the average value of 28° ± 57°), they also may be considered as those containing the βIII-like turn at the D-Trp$_{i+1}$-Lys$_{i+2}$ dipeptide. Overall, both SSTR5-specific conformations of the central tetrapeptide suggested in Table 2 are close to the SSTR3-specific conformation. They differ mostly by the ϕ_{i+3}, Ψ_{i+3} values, which only slightly affect the general shape of the peptide backbone. This similarity is seen in Figure 1. On the other hand, the suggested SSTR4-specific conformation does not contain any β-turn reversals at the D-Trp$_{i+1}$-Lys$_{i+2}$ dipeptide.

Compound 1, SSTR2

Compound 1, SSTR3

Compound 1, SSTR5 (1)

Compound 10, SSTR1

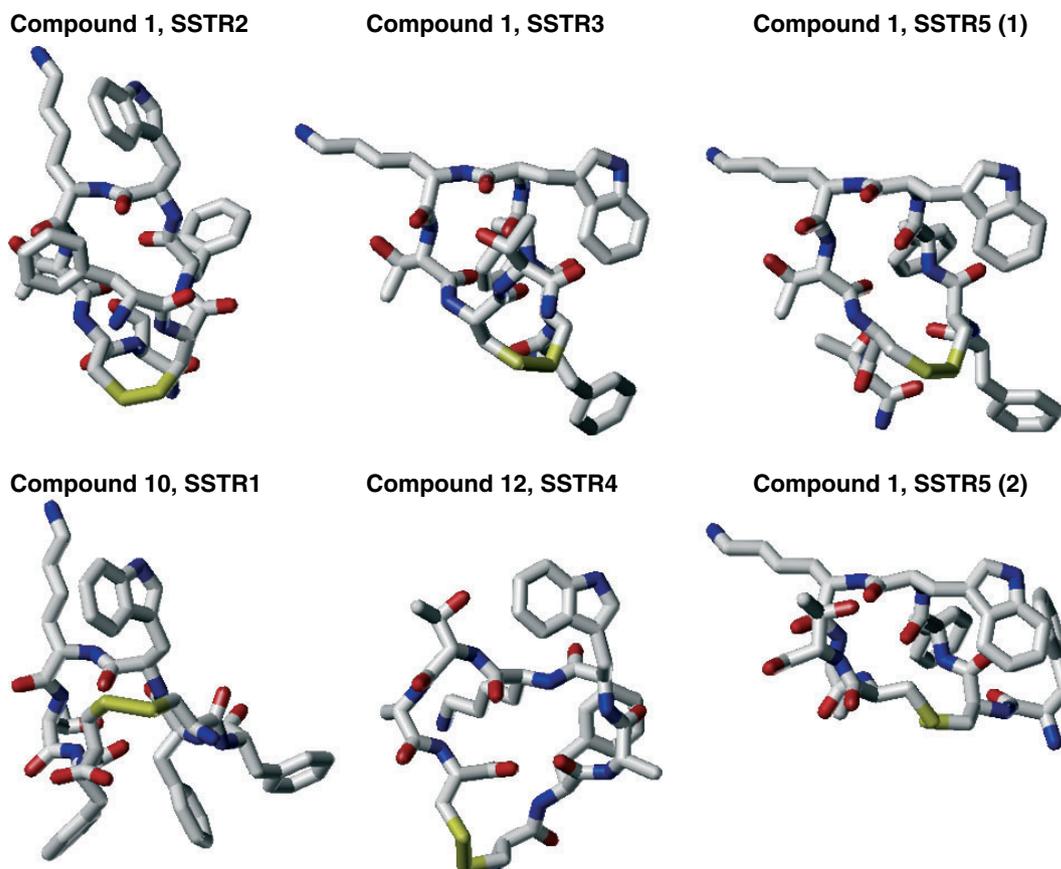**Compound 12, SSTR4**

Compound 1, SSTR5 (2)

Figure 1: Sketches of typical conformations of compounds **1**, **10** and **12** suggested as specifically interacting with different subtypes of SSTRs. All hydrogens are omitted.
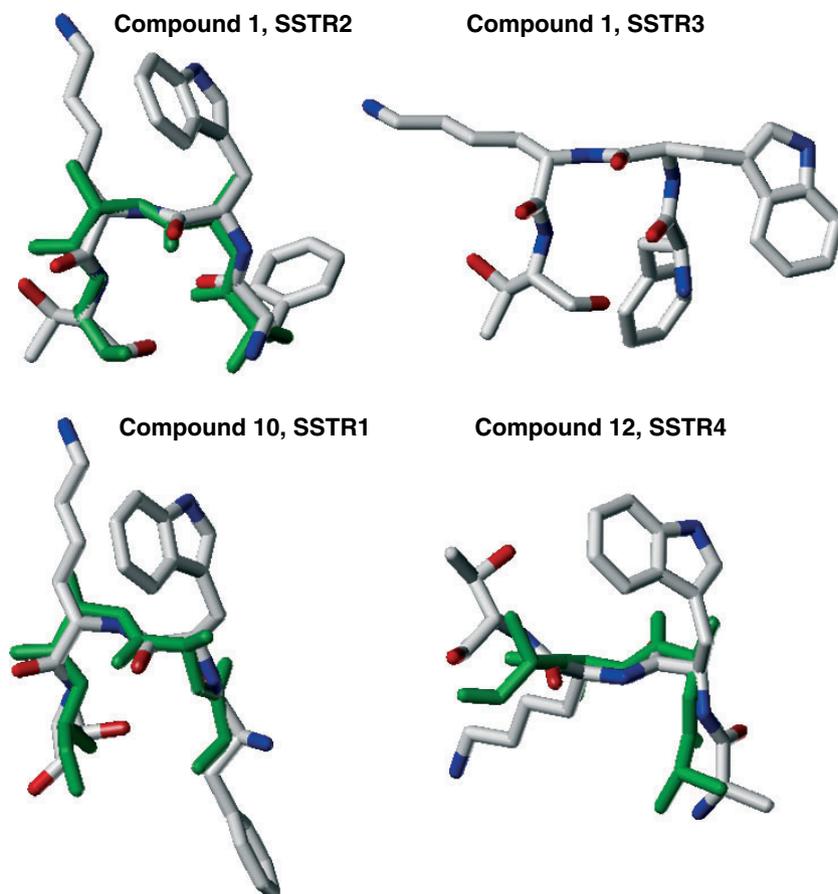
Compound 1, SSTR2　　　　**Compound 1, SSTR3**

Compound 10, SSTR1　　　　**Compound 12, SSTR4**

Figure 2: Sketches of the central tetrapeptides of compounds 1, 10 and 12 corresponding to conformations suggested as specifically interacting with SSTR1-4 (the same as in Figure 1) overlapped with the backbone conformations deduced from NMR measurements [SSTR1, dihedral angles deduced for compound 3 from Table 3 in (11) were used; SSTR2, compound 1, Table 4 (7); SSTR4, compound 8, Table 4 (15)]. NMR-deduced structures are shown in green. All hydrogens are omitted.

Conformations of the peptide backbone for the tetrapeptide Phe/Ala$_i$-D-Trp$_{i+1}$-Lys$_{i+2}$-Thr$_{i+3}$ that were suggested by this study to interact specifically with different subtypes of SSTRs were consistently in good agreement with available experimental data. Recent NMR studies proposed the 3D consensus structures for somatostatin analogs specifically interacting with SSTR1 (11) (see also the PDB entries 1XXZ and 1XY4-9), SSTR2 (7), SSTR3 (17) and SSTR4 (15). The main emphasis of the NMR studies was on establishing specific spatial arrangements of the side chains in and around the central tetrapeptide in DMSO (7,11,15) or water (17) solution. In each case, however, the peptide backbone structures characteristic for several analogs specifically interacting with SSTR1 (11), SSTR2 (7) and SSTR4 (15) (only one analog specific for SSTR3 was investigated (17)) were also determined. The NMR-deduced backbone conformations of the tetrapeptides specific for interactions with SSTR1, SSTR2 and SSTR4 were overlapped with the corresponding conformations suggested by Table 2, yielding good agreement (within the rms cut-off less than 1.2 Å for all heavy atoms including Cβ atoms) for at least one compound considered in the NMR measurements. Figure 2 illustrates how close the backbone conformations suggested by our study (Table 2) and those proposed by NMR measurement (shown in green in Figure 2) converge. We did not find good

consistency between the NMR-deduced conformations for SSTR3-specific analog (17) and the SSTR3-specific conformation from Table 2. In this case, however, deducing the structure from NMR spectra was especially complicated, since two conformers, a major and a minor one, were observed in water. On the other hand, out of two interconverting structures for the SSTR2/5-specific sandostatin proposed by the earlier NMR studies (18) (one with the 'β-sheet' and the other with the 'α-helical' conformation of the central tetrapeptide), the β-sheet structure closely corresponded to our SSTR2-specific conformation from Table 2, and the α-helical structure corresponded to our SSTR3-specific conformation (data not shown). Our results were also very close to the X-ray structure of the SSTR2/5-specific octreotide (19) that revealed the βII' turn at the central D-Trp-Lys dipeptide in close agreement with our SSTR2-specific structure from Table 2.

Conclusions

Our modeling study is the first to suggest different conformations for the peptide backbone of the central tetrapeptide segment that are characteristic for specific interactions of somatostatin-related

peptides with all five different subtypes of SSTRs. These conformations were in good agreement with current experimental data obtained by NMR measurements and X-ray crystallography. They rationalize experimental observations on specificity of interactions of various somatostatin analogs with different subtypes of SSTRs in terms of their mutual conformational interconversion during binding to a specific SSTR subtype. Importantly, these conformations may serve as conformational templates for rational design of non-peptide scaffolds that effectively and selectively interact with different subtypes of SSTRs. Such scaffolds could be used as convenient carriers of radiolabels and near-infrared labels in specific agents for selective diagnostics of tumors based on SSTR subtype overexpression.

Acknowledgments

References

1. Froidevaux S., Eberle A. (2002) Somatostatin analogs and radiopeptides in cancer therapy. Biopolymers;66:161–183.
2. Reubi J.C. (2003) Peptide receptors as molecular targets for cancer diagnosis and therapy. Endocr Rev;24:389–427.
3. Achilefu S., Dorshow R.B., Bugaj J.E., Rajagopalan R. (2000) Novel receptor-targeted fluorescent contrast agents for in vivo tumor imaging. Invest Radiol;35:479–485.
4. Achilefu S., Jimenez H.N., Dorshow R.B., Bugaj J.E., Webb E.G., Wilhelm R.R., Rajagopalan R., Johler J., Erion J.L. (2002) Synthesis, in vitro receptor binding, and in vivo evaluation of fluorescein and carbocyanine peptide-based optical contrast agents. J Med Chem;45:2003–2015.
5. Ye Y., Li W.P., Anderson C.J., Kao J., Nikiforovich G.V., Achilefu S. (2003) Synthesis and characterization of a macrocyclic near-infrared optical scaffold. J Am Chem Soc;125:7766–7767.
6. Janecka A., Zubrzycka M., Janecki T. (2001) Somatostatin analogs. J Pept Res;58:91–107.
7. Grace C.R., Erchegyi J., Koerber S.C., Reubi J.C., Rivier J., Riek R. (2006) Novel sst2-selective somatostatin agonists. Three-dimensional consensus structure by NMR. J Med Chem;49:4487–4496.
8. Rivier J.E., Hoeger C., Erchegyi J., Gulyas J., DeBoard R., Craig A.G., Koerber S.C., Wenger S., Waser B., Schaer J.C., Reubi J.C. (2001) Potent somatostatin undecapeptide agonists selective for somatostatin receptor 1 (sst1). J Med Chem;44:2238–2246.
9. Erchegyi J., Hoeger C.A., Low W., Hoyer D., Waser B., Eltschinger V., Schaer J.C., Cescato R., Reubi J.C., Rivier J.E. (2005) Somatostatin receptor 1 selective analogues: 2. N(alpha)-methylated scan. J Med Chem;48:507–514.
10. Rivier J.E., Kirby D.A., Erchegyi J., Waser B., Eltschinger V., Cescato R., Reubi J.C. (2005) Somatostatin receptor 1 selective analogues: 3. Dicyclic peptides. J Med Chem;48:515–522.
11. Grace C.R., Durrer L., Koerber S.C., Erchegyi J., Reubi J.C., Rivier J.E., Riek R. (2005) Somatostatin receptor 1 selective analogues: 4. Three-dimensional consensus structure by NMR. J Med Chem;48:523–533.
12. Rivier J., Erchegyi J., Hoeger C., Miller C., Low W., Wenger S., Waser B., Schaer J.C., Reubi J.C. (2003) Novel sst(4)-selective somatostatin (SRIF) agonists. 1. Lead identification using a betide scan. J Med Chem;46:5579–5586.
13. Erchegyi J., Penke B., Simon L., Michaelson S., Wenger S., Waser B., Cescato R., Schaer J.C., Reubi J.C., Rivier J. (2003) Novel sst(4)-selective somatostatin (SRIF) agonists. 2. Analogues with beta-methyl-3-(2-naphthyl)alanine substitutions at position 8. J Med Chem;46:5587–5596.
14. Erchegyi J., Waser B., Schaer J.C., Cescato R., Brazeau J.F., Rivier J., Reubi J.C. (2003) Novel sst(4)-selective somatostatin (SRIF) agonists. 3. Analogues amenable to radiolabeling. J Med Chem;46:5597–5605.
15. Grace C.R., Koerber S.C., Erchegyi J., Reubi J.C., Rivier J., Riek R. (2003) Novel sst(4)-selective somatostatin (SRIF) agonists. 4. Three-dimensional consensus structure by NMR. J Med Chem;46:5606–5618.
16. Reubi J.C., Schaer J.C., Wenger S., Hoeger C., Erchegyi J., Waser B., Rivier J. (2000) Sst3-selective potent peptidic somatostatin receptor antagonists. Proc Natl Acad Sci USA;97:13973–13978.
17. Gairi M., Saiz P., Madurga S., Roig X., Erchegyi J., Koerber S.C., Reubi J.C., Rivier J.E., Giralt E. (2006) Conformational analysis of a potent SSTR3-selective somatostatin analogue by NMR in water solution. J Pept Sci;12:82–91.
18. Melacini G., Zhu Q., Goodman M. (1997) Multiconformational nmr analysis of sandostatin (octreotide): equilibrium between beta-sheet and partially helical structures. Biochemistry;36:1233–1241.
19. Pohl E., Heine A., Sheldrick G.M., Dauter Z., Wilson K.S., Kallen J., Huber W., Pfaffli P.J. (1995) Structure of octreotide, a somatostatin analogue. Acta Crystallogr;D51:48–59.
20. Rohrer S.P., Birzin E.T., Mosley R.T., Berk S.C., Hutchins S.M., Shen D.M., Xiong Y. et al. (1998) Rapid identification of subtype-selective agonists of the somatostatin receptor through combinatorial chemistry. Science;282:737–740.
21. Hirschmann R., Hynes J. Jr, Cichy-Knight M.A., van Rijn R.D., Sprengeler P.A., Spoors P.G., Shakespeare W.C., Pietranico-Cole S., Barbosa J., Liu J., Yao W., Rohrer S., Smith A.B., 3rd (1998) Modulation of receptor and receptor subtype affinities using diastereomeric and enantiomeric monosaccharide scaffolds as a means to structural and biological diversity. A new route to ether synthesis. J Med Chem;41:1382–1391.
22. Tran T.T., McKie J., Meutermans W.D., Bourne G.T., Andrews P.R., Smythe M.L. (2005) Topological side-chain classification of beta-turns: ideal motifs for peptidomimetic development. J Comput Aided Mol Des;19:551–566.
23. Hata M., Marshall G.R. (2006) Do benzodiazepines mimic reverse-turn structures? J Comput Aided Mol Des;20:321–331.
24. Dunfield L.G., Burgess A.W., Scheraga H.A. (1978) Energy parameters in polypeptides. 8. Empirical potential energy algorithm for the conformational analysis of large molecules. J Phys Chem;82:2609–2616.
25. Nemethy G., Pottle M.S., Scheraga H.A. (1983) Energy parameters in polypeptides. 9. Updating of geometrical parameters,

nonbonded interactions, and hydrogen bond interactions for the naturally occurring amino acids. J Phys Chem;87:1883–1887.

26. Nikiforovich G.V., Hruby V.J., Prakash O., Gehrig C.A. (1991) Topographical requirements for delta-selective opioid peptides. Biopolymers;31:941–955.

27. Rajeswaran W.G., Hocart S.J., Murphy W.A., Taylor J.E., Coy D.H. (2001) N-methyl scan of somatostatin octapeptide agonists produces interesting effects on receptor subtype specificity. J Med Chem;44:1416–1421.

28. Reubi J.C., Schar J.C., Waser B., Wenger S., Heppeler A., Schmitt J.S., Macke H.R. (2000) Affinity profiles for human somatostatin receptor subtypes sst1-sst5 of somatostatin radiotracers selected for scintigraphic and radiotherapeutic use. Eur J Nucl Med;27:273–282.

29. Rose G.D., Gierasch L.M., Smith J.A. (1985) Turns in peptides and proteins. Adv Protein Chem;37:1–109.